# MULTI-TEMPORAL SAR DATA FILTERING FOR LAND APPLICATIONS

**Urs Wegmüller[(1)], Maurizio Santoro[(1)], and Charles Werner[(1)]**

*[(1)] Gamma Remote Sensing AG, Worbstrasse 225, CH-3073 Gümligen, Switzerland*
*http://www.gamma-rs.ch, wegmuller@gamma-rs.ch*

## ABSTRACT

Multi-temporal SAR data sets are becoming more widely available and show a significant potential for a wide range of applications. This will even more so be the case with the upcoming Sentinel-1 SARs of ESA. Therefore, multi-temporal processing techniques are very relevant. For applications based on SAR backscatter speckle reduction is one important aspect of the processing. In this work we propose a multi-image filtering approach that builds upon multi-image filtering methodologies proposed by Quegan et al. 2001, and structural spatial filtering proposed by Lee et al., 1999. The filtering methodology is described and results are discussed for different satellite SAR sensors.

## 1. INTRODUCTION

Over the last 20 years multi-temporal SAR data sets were acquired in large numbers and over many sites. Related processing techniques were developed and the multi-temporal SAR data showed a significant potential for a wide variety of applications. This will even more so be the case with the upcoming Sentinel-1 SARs of ESA which are designed to achieve global coverage with short repeat intervals. It is important to clearly state here that true acquired coverage and not "potential coverage" is meant. Using a constellation of two satellites and operating these in a special ScanSAR mode permits to achieve complete coverage over land every 6 days or even more frequently if ascending and descending orbit coverage is acquired. As a result, Sentinel-1 will consistently provide excellent multi-temporal data.

For applications based on SAR backscatter in general, and particularly for a mission providing data at about 20m resolution as Sentinel-1, speckle reduction is very essential. For multi-temporal data multi-channel filtering similar to Quegan et al. 2001, shows a very good potential. The main aim of this filtering is to create a set of *M* speckle-reduced images by linearly combining *M* registered images acquired on the same area. In the filter function the input intensity data as well as an estimate of the local mean backscattering coefficient are used:

$$J_i = \frac{\overline{I_i}}{M} \sum_{j=1}^{M} \frac{I_j}{\overline{I_j}} \qquad 1 \le i \le M \qquad (1)$$

where $J_k$ is the filtered output,
$I_i$ are the input intensity data,
$\overline{I_i}$ is the estimate of the local mean backscattering coefficient. It is estimated from the data by averaging intensity values in a local window around each pixel in each image.

In the original method by Quegan et al. 2001, the local mean backscattering coefficient is estimated from the data by averaging intensity values in a local window around each pixel in each image. One possibility to improve this estimation of the local mean backscattering coefficient is to use an adaptive estimator to optimize the trade-off between good reliability of the local estimate and little spatial degradation (Wegmüller et al., 2002). More recently Caves et al., 2011, proposed to design the spatial filter used in the estimation of the spatial averages in the multi-temporal filtering considering not just the scene for which it is applied, but to do this based on the multi-image data stack. In our work presented here we developed such a solution. For the estimation of the spatial averages a multi-temporal structural filter is proposed based on the work of Lee et al., 1999. In the following the filter is introduced and results will be presented and assessed.

## 2. FILTERING METHODOLOGY

### 2.1. Filtering concept

Starting from the above mentioned ideas, we developed a novel multi-scene filtering approach for co-registered backscatter images. A flow chart of this multi-temporal filtering is shown in Figure 1.

The filtering starts from a stack of co-registered backscatter intensity images. Based on these an average image is calculated by a pixel-wise averaging the values through the stack. In this averaging the equivalent number of looks, ENL, increases. ENL is a parameter used to characterize the noise in SAR data, and it is typically estimated for a homogeneous region using

$$ENL = \sqrt{\frac{mean}{stdev}} \qquad (2)$$

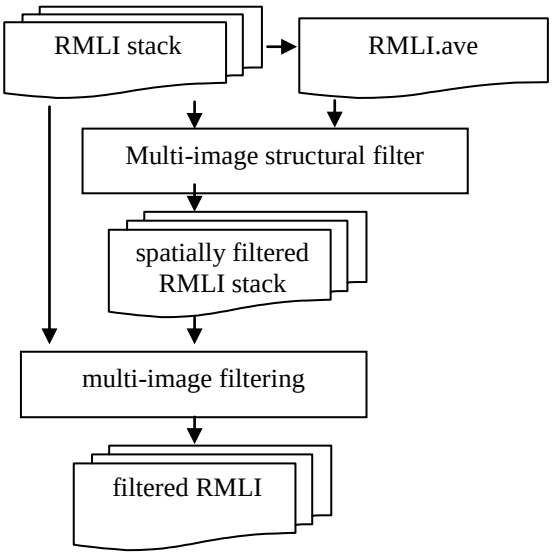


Figure 1 Flow chart of advanced multi-image filtering for stack of co-registered backscatter images. RMLI stands for the co-registered backscatter images.

Both the stack of co-registered unfiltered backscatter intensities and the average image are then inputs to the spatial filtering.

### 2.2. Structural spatial filtering

The structural spatial filtering of multi-image SAR backscatter intensity stacks we developed uses elements of the structural spatial filter as proposed by Lee et al. 1999. The structural spatial filtering by Lee et al. 1999 uses eight structural windows (see Figure 2). In addition to these eight structural windows we use an additional one to include all pixels in the filtering for the case that no clear directionality is identified.

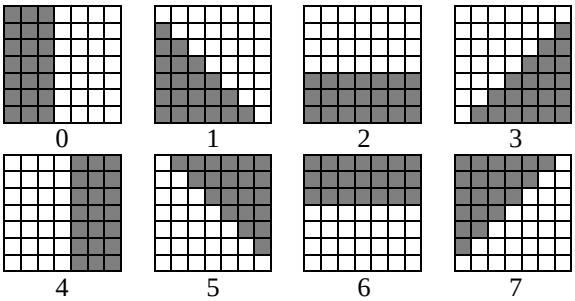


Figure 2 Eight edge-aligned structure windows used in Lee et al. 1999. Pixels in white are used in the filtering.

To determine which structure window is applied for a pixel Lee et al. 1999 determine means for 3 x 3 sub-areas (to reduce the effect of noise) and apply a set of simple edge masks to these sub-area means. The structure window with the maximum value is then used for the spatial filtering.

Here we use an approach with two modifications as compared to Lee et al. 1999. Instead of using an individual image to determine which structural window should be used for the spatial filtering we use the average image. Because of the lower noise of the average image the selection process should be more reliable and it is faster as it is only done once instead of for every image. Furthermore, we compare the maximum value obtained against a threshold. If the maximum is below this threshold we conclude that the images do not show a dominant structure and so we better use the additional homogeneous structure window. As a consequence a higher number of pixels is considered in the filtering of data over homogeneous areas.

The actual weights used in the spatial filtering of the images of the data stack are determined for each scene individually. Using the average image would not be adequate as its statistics are completely different. For a derivation of these weights assuming a multiplicative noise model it is referred to Appendix A of Lee et al., 1999. The filtered value for a pixel at coordinate (i,j) is calculated as a linear combination between the spatial average of the input intensity, $\overline{I_{i,j}}$, and the input intensity at this location, $I_{i,j}$

$$J_{i,j} = (1-b)\overline{I_{i,j}} + bI_{i,j} \qquad (3)$$

The factor *b* is calculated based on the (theoretical) number of looks of the image, *L*, which is determined either using Eq. 2 over homogeneous areas or calculated based on system parameters an multi-looking factors, the spatial average of the input intensity, $\overline{I_{i,j}}$, and the estimated standard deviation of the input intensity estimated for this location, $\sigma_{i,j}$

$$b = \frac{L}{L+1}\left(1 - \frac{\overline{I_{i,j}}^{\,2}}{L\sigma_{i,j}^{\,2}}\right) \qquad (4)$$

In case a negative value is obtained for b it is replaced with 0.0.

### 2.3. Multi-temporal filtering

The spatially filtered images resulting from the structural spatial filtering of the multi-image SAR backscatter intensity stack are then used as the local mean backscattering coefficients required in the multi-image filter function (Eq. 1). The advantage of this approach over the simple spatial average over a box around the filtered image as used in Quegan et al., 2001, is that edges such as field boundaries and strong scatterers are better preserved.

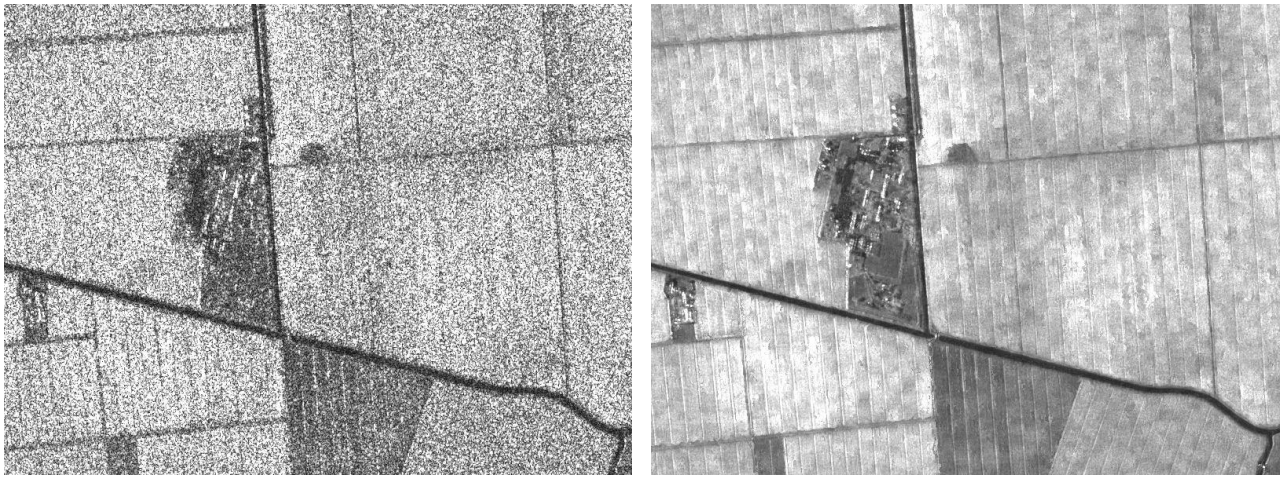

Figure 3 Unfiltered (left) and filtered (right, using the presented advanced multi-temporal filter) 800m x 600m section of a TerraSAR-X Stripmap mode scene over the Po Delta, Italy.

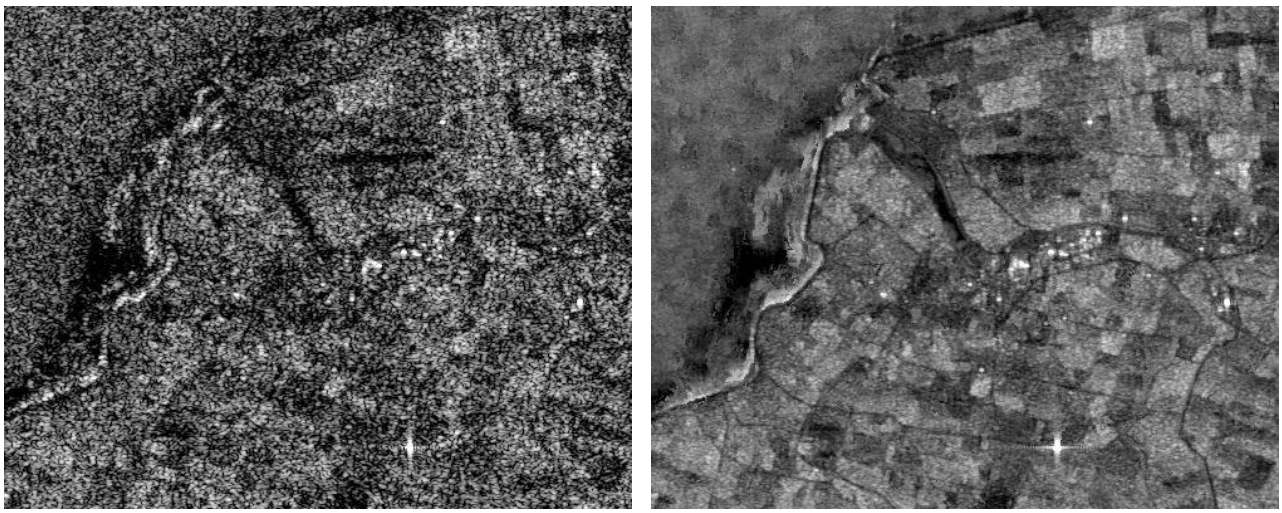

Figure 4 Unfiltered (left) and filtered (right, using the presented advanced multi-temporal filter) Sentinel-1 data for a 5km x 4km section in Zeeland, NL, simulated using a stack ERS-1 ice-phase data.

Figure 5 Unfiltered (left), spatially filtered (center) and filtered using the presented advanced multi-temporal filter(right) PALSAR data for a 4km x 6km section in Hungary.

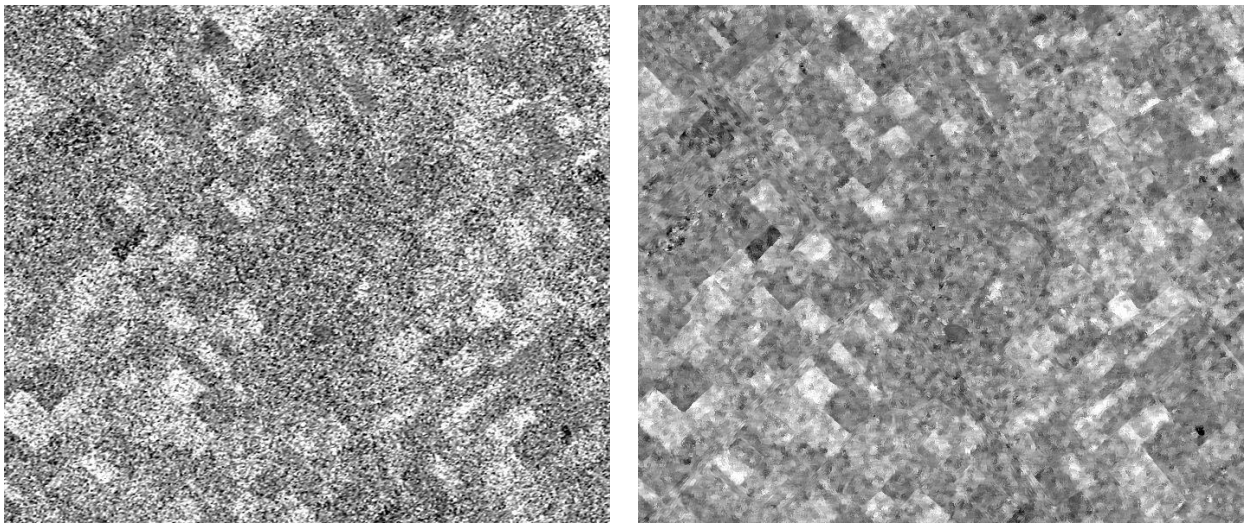

Figure 6 Polarization ratio (HH/VV pol., scale between -6dB and +6dB) calculated for the AGRISAR'09 RSAT-2 scene acquired on 9-Jul-2009 over Flevoland, NL (section of 7km x 6km). The ratio shown to the left is calculated from the unfiltered MLI, the ratio to the right from the advanced multi-temporally filtered MLI.

## 3. ASSESSMENT OF RESULTS

We assessed the filtering performance using stacks of more than 25 scenes of ERS data, Radarsat-2 data from the AgriSAR'09 Campaign (Caves et al., 2011), PALSAR data and TerraSAR-X data.

In the multi-image filtering, an assumption used is that the spatial patterns remain unchanged over time. This is often almost perfectly the case for agricultural fields, built up structures as houses, roads, power lines, dams and alike also meet this criteria. As a consequence, the filter performs well over these targets with a significant increase of the Equivalent Number of Looks (ENL) over homogeneous areas such as fields while maintaining individual scatterers and field boundaries sharp. In areas with varying geometries (e.g. in tidal zones, or for vehicles), where the assumption of temporally stable geometries is not met for all boundaries and bright targets, we can observe cases where the proposed filtering is not optimal but overall the results still look quite reasonable also in these cases.

Applying the structural filter in the estimation of the spatial averages used in the temporal filtering is particularly attractive when working at high spatial resolutions with a low number of looks per pixel as it permits getting high resolution (for a given sensor) results with reasonable look numbers. Figure 3 shows a small section of an unfiltered and temporally filtered scene of a TerraSAR-X stack demonstrating the visual improvement from the filtering. What is more relevant for applications is that the ENL is increased by more than a factor 10 which is very relevant when applying algorithms. Applications as soil moisture monitoring, crop parameter retrieval, classification and change detection can strongly benefit when working at pixel level. The main advantages over the standard multi-temporal filter by Quegan et al., 2001 are the much more local transition between different backscatter levels e.g. between adjacent fields and that strong individual scatterers remain better focused. On the other hand, the standard method results in slightly higher ENL values because a larger number of pixels is considered in the estimation of the spatial averages used in the multi-temporal filtering.

Applying azimuth spectrum band-pass filtering to ERS-1 data acquired in the ice-phase mode with 3-day repeat cycles we simulated data with similar characteristics as for the Sentinel-1 interferometric Wide Swath mode and applied the advanced multi-temporal filter. The results (see Figure 4) confirm that a significant improvement can be achieved. The ENL increased over fields from about 1.5 to about 10.

For a stack of 22 PALSAR backscatter images, considering FBS and FBD mode data, a section of one image is shown unfiltered, spatially filtered using the above described multi-temporal version of the structural spatial filtering, and the proposed multi-temporal filtering. Both the spatial filtering and the multi-temporal filtering significantly increase the ENL from about 3 to about 15. In the area of the villages and for the field boundaries the result is "sharper" for the proposed multi-temporal filtering as compared to the spatial filtering.

For the AGRISAR'09 data over Flevoland (Caves et al., 2011) we also applied the proposed multi-temporal filtering. In this case the data are from different tracks and different polarizations are available. In a first step all SLC were co-registered to a reference of the same

track, then multi-looked with 2 range and 3 azimuth looks and then geocoded to a 10m sampling. A total of 240 (4 x 60) co-registered geocoded backscatter data sets were then available. For the multi-temporal filtering a spatial window size of 7 pixels was used. With the proposed multi-temporal filtering the ENL increased from about 4 to 32. To assess the impact of the temporal filtering on the calculation of backscatter ratios we calculated polarization ratios from the unfiltered as well as the filtered data (Figure 6). A high HH/VV polarization ratio (>> 0 dB) at this time of the year is an indication for a "wheat-like" structure (HH scattering from ground is less attenuated in the primarily vertical canopy). The effect of the filtering on the polarization ratio image is obvious.

## 4. CONCLUSIONS

A novel multi-image filtering approach was presented. The approach is based on the multi-temporal filter by Quegan et al., 2001 but uses a different method to estimate the spatial averages used in the filter function. It is proposed to use a special structural filter to estimate these spatial averages. Given that a multi-image data set is available the determination of the filter structure is improved and made more efficient by determining it based on the average image. The filtering was applied to data stacks of various sensors permitting to increase the ENL significantly while maintaining a good spatial resolution.

## 5. REFERENCES


Caves R., G. Davidson, J. Padda, and A. Ma, ESA Contract 22689/09/NL/FF/ef, Final Report Vol. 2 Data Analysis – Multi-Temporal Filtering, 2011.

Lee J-S., M.R. Grunes, and G. de Grandi, Polarimetric SAR Speckle Filtering and Its Implication for Classificantion, IEEE TGRS, Vol.. 37, No. 5, pp. 2363-2373, 1999.

Quegan and Yu, Filtering of multichannel SAR images, IEEE Trans Geosci. and Remote Sensing, vol. 39, no. 11, 2001.

Wegmüller U., A. Wiesmann, T. Strozzi, and C. Werner, Forest mapping with multi-temporal SAR, Proc. ForestSAT'02 Conf. Edinburgh, Scotland, 5.-9. Aug. 2002.


## 6. ACKNOWLEDGMENT


This work was supported by ESA ESTEC Contract 4000104365. ERS, ENVISAT data courtesy ESA. SAR data used. MDA and ESA are acknowledged for the access to the AGRISAR'2009 Campaign Radarsat-2 SAR data used. PALSAR data courtesy JAXA RA Project 094. TerraSAR-X data courtesy LAN0242, ©DLR.